

Probing inflationary features with galaxy ultraviolet luminosity function observables

Sandeep Kumar Acharya^{a,1}

^a*Indian Institute of Astrophysics, Koramangala II Block, Bengaluru 560 034, India*

E-mail: sandeepkumaracharya92@gmail.com

ABSTRACT: We use the galaxy ultraviolet luminosity function measurements at $z = 6 - 9$ to constrain modification to standard inflationary power spectrum. These observables are sensitive to the matter power spectrum which itself depends on inflationary initial conditions. We consider specific models where a bump or oscillatory features are introduced to the standard power law inflation spectrum. We find that the galaxy luminosity observables can probe such modifications at wavenumbers $0.5 \lesssim k \lesssim 20 \text{ Mpc}^{-1}$. We obtain upper limits on the amplitude of bump-like features at the mentioned wavenumbers. We obtain constraints which are similar to previous constraints on these models using measurements of optical depth of reionization. However, the galaxy luminosity functions are a more direct probe for these type of models and, therefore, can complement indirect constraints coming from measurements of IGM properties.

¹Corresponding author.

1 Introduction

The understanding of properties and distribution of galaxies at high redshifts, especially during reionization epoch ($z \gtrsim 6$), has become a subject of significant interest in recent years. With the surge of observational data from large galaxy surveys, we are beginning to test our theoretical understanding of high redshift galaxy formation, developed over last couple of decades [1–8]. While measurements of Cosmic Microwave Background (CMB) [9–12] and large scale structure (LSS) [13, 14] have established our understanding of the Universe on larger length scales ($\gtrsim 1 - 10$ Mpc), these high redshift galaxies provide a complementary probe on smaller length scales.

One such high redshift observable is galaxy ultraviolet luminosity function (UVLF) which is defined as the comoving number density of galaxy per unit luminosity. These measurements are made at rest frame wavelength of about 1500\AA . The observed luminosity provides a proxy for the inference of star formation rate which captures information regarding galaxy formation and their cosmological evolution. The Hubble Space Telescope (HST) has measured UVLFs upto $z \approx 10$ [15–17]. Recently, James Webb Space Telescope (JWST) has pushed this limit to $z \approx 15$ [18–21]. These measurements have inferred a large abundance of UV bright galaxies as compared to the prediction from standard galaxy formation model in Λ CDM framework extrapolated to these redshifts [22–27]. Several proposals beyond Λ CDM cosmology, higher star formation efficiency as well as stochasticity of bright UV galaxies have been proposed [28–38] to alleviate this problem. More recent works [39, 40] show that JWST data necessitates evolving star formation efficiency as a function of redshift within Λ CDM framework.

The UVLF observables have also been used to probe particle nature of dark matter [41–45]. Non-trivial particle interaction of dark matter beyond cold dark matter paradigm modifies the shape of matter power spectrum. This modification imprints its characteristic signature on halo mass function which captures the comoving number density of dark matter halo as a function of halo mass. Since the dark matter halos act as host for galaxies, the number density of galaxies including total star formation rate in the universe is also modified. Therefore, UVLF measurements which constrain star formation can indirectly test interaction properties of dark matter. Further, the matter power spectrum also captures information regarding initial condition or inflationary power spectrum [46–49] of the Universe. Therefore, these observables can be used to probe modification to our understanding of inflation even within standard Λ CDM framework. Current CMB and LSS measurements are consistent with inflation power spectrum being a featureless power law within wavenumber $10^{-4} \text{ Mpc}^{-1} \lesssim k \lesssim 0.1 \text{ Mpc}^{-1}$ [9–14]. However, several models predict scale dependent features [50–55] which can modify the power spectrum at $k \gtrsim 0.1 \text{ Mpc}^{-1}$.

In this paper, we probe the effect of modified inflationary power spectrum on the UVLF observables. We consider a specific model which introduces a bump-like feature on top of power law spectrum due to particle production during inflation [56–60]. These models have been studied in the context of CMB observables [61] and galaxy two point correlation function [62] and upper limits on the amplitude of such features have been obtained within $10^{-4} \text{ Mpc}^{-1} \lesssim k \lesssim 0.1 \text{ Mpc}^{-1}$ regime. Recently, this model was studied in the context of predictions for 21cm observables [63, 64]. It was shown that global 21cm signal can constrain these features at wavenumbers $0.1 \text{ Mpc}^{-1} \lesssim k \lesssim 10$

Mpc⁻¹. In this work, we show that available UVLF data can already constrain the amplitude of bump like features at these larger wavenumbers.

This paper is organized as follows. We describe our modelling of UVLF data in Sec. 2. Our formalism for modified inflationary power spectrum is described in Sec. 3. We provide our results on these modified power spectrum in Sec. 4. We study a couple of cases on inflation with oscillatory features in Sec. 5. We conclude in Sec. 6. Throughout the work, we use the best fit cosmological parameters obtained from *Planck* experiment [10].

2 Theoretical modelling of UVLF

In order to theoretically model star formation inside galaxies, we use the formalism of halo model [65, 66]. In this formalism, the dark matter halos provide gravitational potential well for baryons to fall into after decoupling from CMB photons. Therefore, the baryonic tracers such as distribution of galaxies are expected to be somewhat of a proxy of dark matter distribution as well as its particle properties. In order to compute star formation, we first assign galaxies to dark matter halos. We assume that each dark matter halo hosts one galaxy, similar to the modelling done in [39, 40]. This is motivated by the fact that at $z \gtrsim 6$, massive dark matter halos which can host multiple galaxies are increasingly rare. The stellar mass of galaxy (M_*) can be related to the mass of dark matter halo (M_h) as [39, 40, 67–69],

$$M_* = f_*(M_h) \left(\frac{\Omega_b}{\Omega_m} \right) M_h, \quad (2.1)$$

where f_* is the star formation efficiency which is parameterized as,

$$f_*(M_h) = f_{*,10} \left(\frac{M_h}{10^{10} M_\odot} \right)^{\alpha_*} \quad (2.2)$$

The star formation rate (SFR) is given by,

$$\dot{M}_*(M_h, z) = \frac{M_*(M_h)}{t_*(z)}, \quad (2.3)$$

where $t_*(z)$ is the timescale of star formation which we assume to be Hubble scale or $t_*(z) = 1/H(z)$. There can be O(1) numerical factor in the above relation which can be absorbed within $f_{*,10}$. Altogether, the expression for SFR becomes,

$$\dot{M}_* = f_{*,10} H(z) \left(\frac{M_h}{10^{10} M_\odot} \right)^{\alpha_*} \left(\frac{\Omega_b}{\Omega_m} \right) M_h \quad (2.4)$$

The luminosity of galaxy at rest frame wavelength 1500Å can be related to its SFR via the scaling relation,

$$\mathcal{K}_{UV} = \frac{\dot{M}_*(M_h, z)}{L_{UV}}, \quad (2.5)$$

which is tuned to observations at low redshifts and with the assumption of Salpeter IMF [70]. We assume a fiducial value of $\mathcal{K}_{UV} = 1.15485 \times 10^{-28} M_\odot \text{ yr}^{-1} / \text{ergs s}^{-1} \text{ Hz}^{-1}$. Therefore, the UV

luminosity can be expressed as,

$$L_{UV} = \frac{f_{*,10}}{\mathcal{K}_{UV}} H(z) \left(\frac{M_h}{10^{10} M_\odot} \right)^{\alpha_*} \left(\frac{\Omega_b}{\Omega_m} \right) M_h \quad (2.6)$$

We can relate the luminosity to the UV magnitude using the relation,

$$\log_{10} \left(\frac{L_{UV}}{\text{ergs s}^{-1} \text{ Hz}^{-1}} \right) = 0.4 \times (51.6 - M_{UV}) \quad (2.7)$$

Finally, the UVLF or the number density of galaxies as a function of their luminosity or magnitude is given by,

$$\Phi_{UV}(z, M_{UV}) = \frac{dn}{dM_{UV}} = \frac{dn}{dM_h} \frac{dM_h}{dL_{UV}} \frac{dL_{UV}}{dM_{UV}} \quad (2.8)$$

The halo mass function $\frac{dn}{dM_h}$ encodes the comoving number density of dark matter halos in the mass range M_h and $M_h + dM_h$. It is a function of variance of matter density field $\sigma(M_h, z)$ and is given by [71],

$$\frac{dn}{d \ln M_h} = \frac{\rho_m}{M_h} \frac{d \ln \sigma^{-1}}{d \ln M_h} f(\sigma, z), \quad (2.9)$$

where ρ_m is the average matter energy density today. In this work, we use the fitting function $f(\sigma, z)$ provided by Jenkins et al [72]. Further, $\sigma(M_h, z) = \sigma(M_h) D(z)$, where $D(z)$ is the growth factor. The smoothed variance $\sigma(M_h)$ is expressed as,

$$\sigma(R) = \frac{1}{2\pi^2} \int_0^\infty dk k^2 P_m(k) W^2(kR), \quad (2.10)$$

where $P_m(k)$ is the matter power spectrum, $W(kR)$ is top-hat smoothing function in R or position space and $M_h = \frac{4\pi}{3} \rho_m R^3$.

3 Modification to matter power spectrum due to inflationary bump like feature

The standard inflationary power spectrum is given by,

$$P_s(k) = A_s \left(\frac{k}{k_*} \right)^{n_s - 1}, \quad (3.1)$$

with $k_* = 0.05 \text{ Mpc}^{-1}$, A_s and n_s parameterizes the amplitude and slope of power law. They are tightly constrained by CMB data [10] with values $\ln(10^{10} A_s) = 3.044 \pm 0.014$, $n_s = 0.9649 \pm 0.0042$. Bursts of particle production during inflation can generate bump-like features in the power spectrum [56–60]. We parameterize the modified power spectrum by including the dominant term as [59, 63],

$$P_s(k) = A_s \left(\frac{k}{k_*} \right)^{n_s - 1} + A_I \sum_i \left(\frac{f_1(x_i)}{f_1^{\max}} \right) \quad (3.2)$$

The function $f_1(x)$ is expressed as,

$$f_1(x_i) = \frac{[\sin(x_i) - \text{SinIntegral}(x_i)]^2}{x_i^3}, \quad (3.3)$$

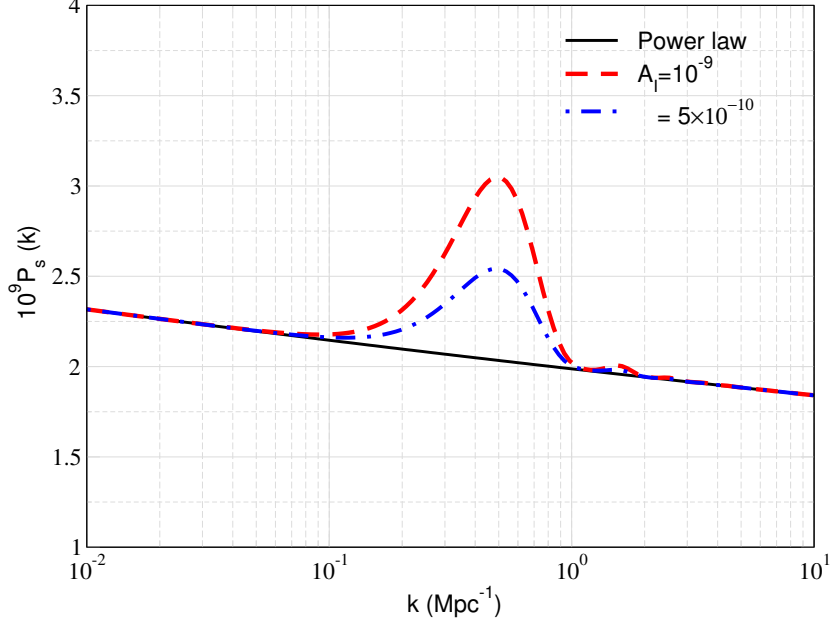


Figure 1: Modified inflationary power spectrum with a single bump like feature, $k_{\text{peak}} = 0.5 \text{ Mpc}^{-1}$ and amplitude as denoted in the plot. We plot the standard power law spectrum in black with parameters as denoted in the text.

where $x_i = \frac{k}{k_i}$ and f_1^{max} is the maximum value of $f_1(x)$. The parameter k_i is related to the position of i th feature which peaks at $k_{\text{peak},i} = 3.35k_i$. For simplicity, we consider one bump or $i = 1$ in this work. In Fig. 1, we plot the modified power spectrum with $k_{\text{peak}} = 0.5 \text{ Mpc}^{-1}$ for a couple of cases. We plot the corresponding $\sigma(M_h)$ in Fig. 2. We compute the modified matter power spectrum as $P_m(k) = P_s(k)\mathcal{T}^2(k)$, where $\mathcal{T}(k)$ is the matter transfer function computed using CLASS [73]. We substitute the matter power spectrum in Eq. 2.10 in order to compute $\sigma(M_h)$. We find that $\sigma(M_h)$ changes non-negligibly which will be further magnified in the halo mass function due to its exponential dependence on $\sigma(M_h)$ [72].

4 Analysis and results

We use the UVLF measurements within the redshift range 6 to 9 to do our analysis. We have not used JWST data at higher redshifts. Recent analysis [39, 40] show that these data require significant redshift evolution of star formation efficiency f_* which require more complex modelling. In this work, we do not take the redshift evolution of f_* into account. Further, we use the data points within $M_{\text{UV}} \in [-21, -16]$. We note that lower M_{UV} corresponds to larger, heavier or more luminous galaxies. These are more susceptible to absorption by dust which result in break in slope at $M_{\text{UV}} \lesssim -21$ (Left panel of Fig. 3). Also, at higher mass, baryonic feedback effects may be important which may not be captured by our simple model.

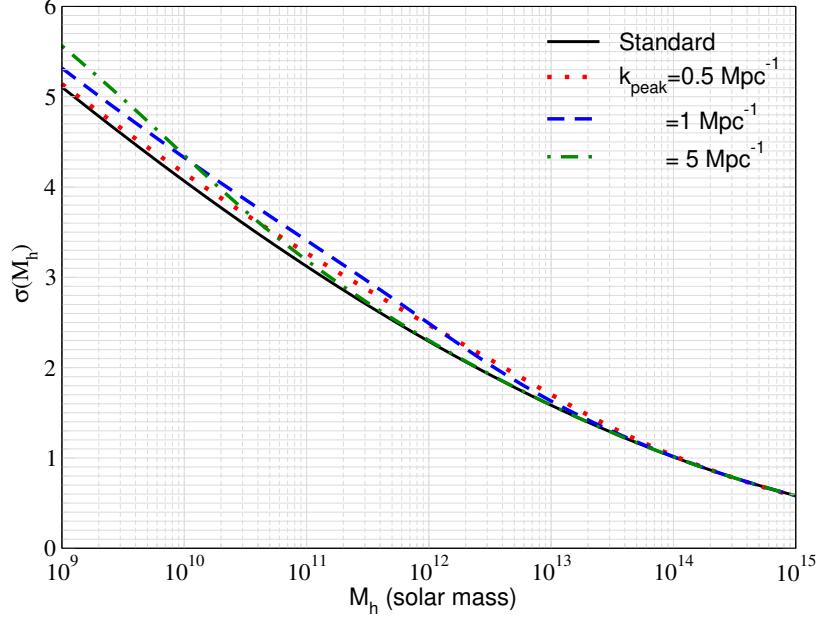


Figure 2: $\sigma(M_h)$ as a function of halo mass at $z = 0$ for different k_{peak} and $A_I = 10^{-9}$. We have chosen the normalization $\sigma_8 = 0.8111$ [10] for all the curves. We note that σ_8 is a derived parameter and a choice of A_s or σ_8 fixes the other one.

First, we fit our standard case with $A_I = 0$ to the UVLF data. We have used MCMC sampling to obtain the fit. We obtain best fit parameters $f_{*,10} = 0.094^{+0.036}_{-0.044}$ and $\alpha_* = 0.39^{+0.15}_{-0.22}$ within 1σ confidence. We plot this best fit to the data at $z = 6$ in the right panel of Fig. 3. Next we consider cases with few different k_{peak} and $A_I = 10^{-9}$. We find that we are in a position to constrain these cases with presently available UVLF data.

Then, we perform the full calculation with the bump like feature. We choose flat prior on $f_{*,10} \in [0.05, 0.2]$, $\alpha_* \in [0.2, 0.6]$ and $A_I \in [10^{-9}, 10^{-6}]$. Our constraints are plotted in Fig. 4. Our constraints cover range $k \in [0.3 - 20]$ Mpc^{-1} . At larger length scales or smaller k , CMB anisotropy provides the strongest constraint. Our constraints are competitive with those derived from CMB optical depth or τ_{Planck} [63] in the relevant range of k . We note that to obtain the τ constraint, a fiducial astrophysical model with fixed parameter values were assumed. Further, τ is related to the ionization history of the Universe which depends on the Intergalactic medium (IGM) properties. Ionizing photons from stars inside the smallest galaxies, which are too faint to see, escape to IGM and affect the ionization history of the Universe. Therefore, the τ constraint is an indirect probe of galaxy properties and capture the cumulative effect of smallest to largest galaxies. However, UVLFs are a more direct probe of galaxy properties as in we directly observe light from these galaxies as a function of their luminosity (Fig. 3). Therefore, we will not be able to constrain properties of smaller, faint galaxies which are not observable (for example, $M_{\text{UV}} \gtrsim -16$ in Fig. 3). The UVLF constraint becomes weaker compared to the τ constraint at high k in Fig. 4 due to this effect. We note that our UVLF constraints can complement optical depth as well as 21cm constraints that will come in future.

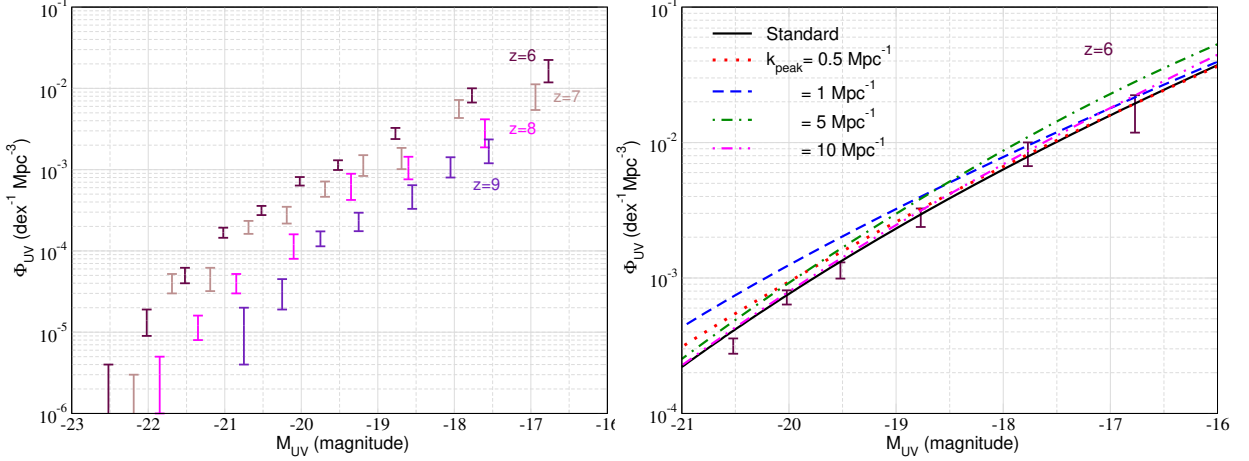


Figure 3: (a) Left panel: UVLF measurements as a function of luminosity or magnitude for a few different redshifts. For $z = 6 - 8$, we use the result of [15] while for $z = 9$, we use the data from [18]. (b) Right panel: Theoretical prediction for UVLF at $z = 6$ for different k_{peak} and $A_I = 10^{-9}$. We have used $f_{*,10} = 0.1$ and $\alpha_* = 0.4$ which are the best fit parameters to the data in the standard case with $A_I = 0$ (drawn in solid black).

5 Inflation power spectrum with damped oscillations

In this section, we briefly consider a scenario with oscillatory features in inflationary power spectrum. These models have been motivated and studied in [74–78]. We use the parameterization provided in [78] with a simple modification. The expression for power spectrum with linear damped oscillation is given by,

$$P_s(k) = A_s \left(\frac{k}{k_*} \right)^{n_s-1} \left[1 + \alpha \cos\left(\omega \frac{k}{k'} + \phi\right) e^{-\frac{\beta^2(k-\mu)^2}{2k'^2}} e^{-\frac{0.25}{k^2}} \right], \quad (5.1)$$

while log damped oscillation is given by,

$$P_s(k) = A_s \left(\frac{k}{k_*} \right)^{n_s-1} \left[1 + \alpha \cos\left(\omega \ln \frac{k}{k'} + \phi\right) e^{-\frac{\beta^2(k-\mu)^2}{2k'^2}} e^{-\frac{0.25}{k^2}} \right] \quad (5.2)$$

We have added an extra factor of $e^{-0.25/k^2}$ to damp out the oscillations at low k . The four parameters, α, ω, k', ϕ set the amplitude, period, wavenumber and phase of oscillatory feature while β is the damping factor at high k . A detail exploration over the parameter space is beyond the scope of this work. However, we study a couple of cases by fixing the parameters such as, $\phi = 0, \beta = 5, \mu = 0.01, k' = 50 \text{ Mpc}^{-1}$. Some of these parameter choices are motivated by the values used in [78]. We also find that α has to be $\lesssim 1$ so that $P_s(k)$ does not turn negative. We show the modified power spectrum and corresponding σ for a couple of cases in Fig. 5. For linear damped case, we see a significant deviation of $\sigma(M_h)$ from standard case. Due to sharper oscillations in log damped case, the integral in Eq. 2.10 averages out and is similar to standard case though some residual oscillatory pattern can be seen.

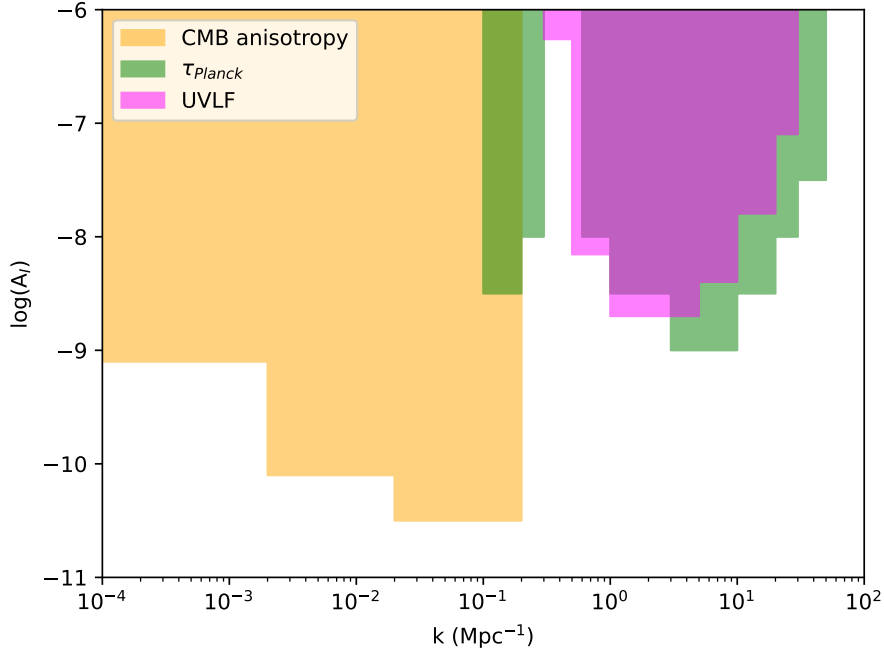


Figure 4: Constraints on A_I (at 95 percent confidence interval) as a function of scale from different probes as denoted in the plot. Our new constraints cover range between $k \in [0.3 - 20] \text{ Mpc}^{-1}$. Our constraints are competitive with constraints derived from CMB optical depth τ_{Planck} [63]. In deriving the optical depth constraint, a fiducial astrophysical model with fixed parameter values was assumed.

We plot the prediction for UVLFs for these scenarios in Fig. 6. We have used the best fit value for $f_{*,10} = 0.1$ and $\alpha_* = 0.4$. We find that linear damped case with $\alpha = 0.5$ may be ruled out assuming a fixed star formation efficiency parameters. However, the log damped case may not be ruled out even for amplitude close to highest possible values.

6 Conclusions

In this work, we constrain modification to inflationary power spectrum at wavenumbers $0.3 \lesssim k \lesssim 20 \text{ Mpc}^{-1}$ using galaxy UVLF data within redshift range of 6 to 9. The strongest constraint corresponds to $A_I \sim 10^{-9}$ for $k_{\text{peak}} \in [1 - 5] \text{ Mpc}^{-1}$. Our constraints are complementary to previously obtained constraint using optical depth of reionization. However, UVLFs are a more direct probe as they directly count the number of galaxies as opposed to indirect effect of galaxies on the IGM.

The analysis presented here makes some simplifying assumptions which can be further improved in future with more data. Our star formation modelling assumes a simple power law with a scaling relation tuned to low redshift measurements. Any redshift evolution in these scaling relation can complicate the inference on inflation power spectrum. Complementary cosmological observables

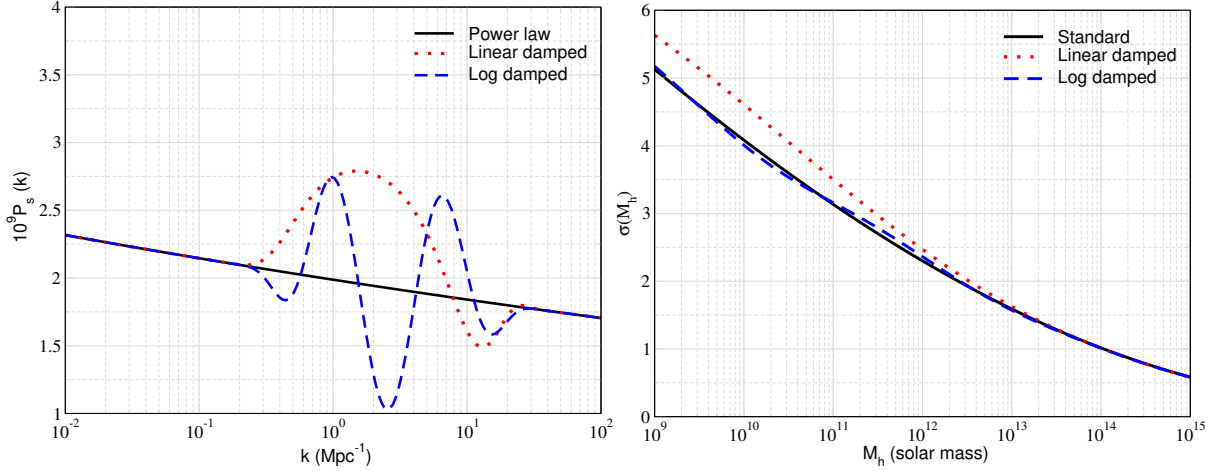


Figure 5: (a) Left panel: Modified inflationary power spectrum with linear and log-damped oscillatory features. For linear-damped case, the parameters are $\alpha = 0.5$, $\log_{10}\omega = 1$ while for log-damped case we use $\alpha = 0.5$, $\log_{10}\omega = 0.5$. We use $k' = 50 \text{ Mpc}^{-1}$, $\beta = 5$, $\mu = 0.01$ for both cases. (b) Right panel: variance $\sigma(M_h)$ with the normalization $\sigma_8 = 0.8111$.

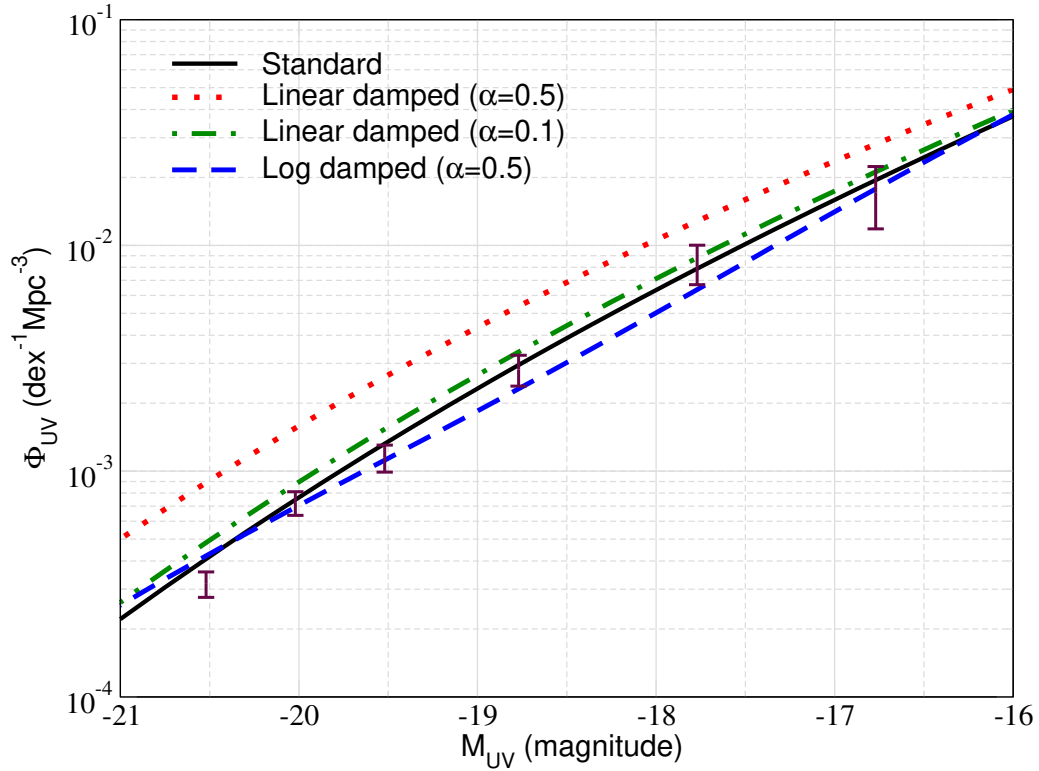


Figure 6: Comparison of UVLF data at $z = 6$ for few cases studied in Fig. 5. We have used the best fit parameters for star formation efficiency $f_{*,10} = 0.1$, $\alpha_* = 0.4$.

such as 21cm global, power spectrum and intensity mapping experiments should also be sensitive to inflation power spectrum as well as star formation. A joint modelling of all these observables may further reduce the uncertainties in astrophysical modelling and tighten up the constraints or result in a detection.

Acknowledgements

We acknowledge discussions with Prof Pravabati Chingangbam during the course of this work.

References

- [1] R. Barkana and A. Loeb. In the beginning: the first sources of light and the reionization of the universe. *Physics Reports*, 349(2):125–238, July 2001. [arXiv:astro-ph/0010468](#), [DOI], [ADS].
- [2] Michael Boylan-Kolchin, Volker Springel, Simon D. M. White, Adrian Jenkins, and Gerard Lemson. Resolving cosmic structure formation with the Millennium-II Simulation. *MNRAS*, 398(3):1150–1164, September 2009. [arXiv:0903.3041](#), [DOI], [ADS].
- [3] Andrei Mesinger, Steven Furlanetto, and Renyue Cen. 21CMFAST: a fast, seminumerical simulation of the high-redshift 21-cm signal. *MNRAS*, 411(2):955–972, February 2011. [arXiv:1003.3878](#), [DOI], [ADS].
- [4] Mark Vogelsberger, Shy Genel, Volker Springel, Paul Torrey, Debora Sijacki, Dandan Xu, Greg Snyder, Dylan Nelson, and Lars Hernquist. Introducing the Illustris Project: simulating the coevolution of dark and visible matter in the Universe. *MNRAS*, 444(2):1518–1547, October 2014. [arXiv:1405.2921](#), [DOI], [ADS].
- [5] Joop Schaye, Robert A. Crain, Richard G. Bower, Michelle Furlong, Matthieu Schaller, Tom Theuns, Claudio Dalla Vecchia, Carlos S. Frenk, I. G. McCarthy, John C. Helly, Adrian Jenkins, Y. M. Rosas-Guevara, Simon D. M. White, Maarten Baes, C. M. Booth, Peter Camps, Julio F. Navarro, Yan Qu, Alireza Rahmati, Till Sawala, Peter A. Thomas, and James Trayford. The EAGLE project: simulating the evolution and assembly of galaxies and their environments. *MNRAS*, 446(1):521–554, January 2015. [arXiv:1407.7040](#), [DOI], [ADS].
- [6] Pratika Dayal and Andrea Ferrara. Early galaxy formation and its large-scale effects. *Physics Reports*, 780:1–64, December 2018. [arXiv:1809.09136](#), [DOI], [ADS].
- [7] Peter Behroozi, Charlie Conroy, Risa H. Wechsler, Andrew Hearin, Christina C. Williams, Benjamin P. Moster, L. Y. Aaron Yung, Rachel S. Somerville, Stefan Gottlöber, Gustavo Yepes, and Ryan Endsley. The Universe at $z \lesssim 10$: predictions for JWST from the UNIVERSEMACHINE DR1. *MNRAS*, 499(4):5702–5718, December 2020. [arXiv:2007.04988](#), [DOI], [ADS].
- [8] Barun Maity and Tirthankar Roy Choudhury. Probing the thermal history during reionization using a seminumerical photon-conserving code SCRIPT. *MNRAS*, 511(2):2239–2258, April 2022. [arXiv:2110.14231](#), [DOI], [ADS].
- [9] E. Komatsu, K. M. Smith, J. Dunkley, C. L. Bennett, B. Gold, G. Hinshaw, N. Jarosik, D. Larson, M. R. Nolta, L. Page, D. N. Spergel, M. Halpern, R. S. Hill, A. Kogut, M. Limon, S. S. Meyer, N. Odegard, G. S. Tucker, J. L. Weiland, E. Wollack, and E. L. Wright. Seven-year Wilkinson Microwave Anisotropy Probe (WMAP) Observations: Cosmological Interpretation. *ApJS*, 192(2):18, February 2011. [arXiv:1001.4538](#), [DOI], [ADS].

- [10] Planck Collaboration et al. Planck 2018 results. VI. Cosmological parameters. *A&A*, 641:A6, September 2020. [arXiv:1807.06209](#), [DOI], [ADS].
- [11] The Atacama Cosmology Telescope collaboration. The Atacama Cosmology Telescope: DR6 power spectra, likelihoods and Λ CDM parameters. *JCAP*, 2025(11):062, November 2025. [arXiv:2503.14452](#), [DOI], [ADS].
- [12] SPT collaboration. SPT-3G D1: CMB temperature and polarization power spectra and cosmology from 2019 and 2020 observations of the SPT-3G Main field. *arXiv e-prints*, page arXiv:2506.20707, June 2025. [arXiv:2506.20707](#), [DOI], [ADS].
- [13] Alam et al (eBOSS). Completed SDSS-IV extended Baryon Oscillation Spectroscopic Survey: Cosmological implications from two decades of spectroscopic surveys at the Apache Point Observatory. *Phys.Rev.D*, 103(8):083533, April 2021. [arXiv:2007.08991](#), [DOI], [ADS].
- [14] S. Novell-Masot, H. Gil-Marín, L. Verde, J. Aguilar, S. Ahlen, S. Bailey, S. BenZvi, D. Bianchi, D. Brooks, E. Buckley-Geer, A. Carnero Rosell, E. Chaussidon, T. Claybaugh, S. Cole, A. Cuceu, K. S. Dawson, A. de la Macorra, R. Demina, A. Dey, B. Dey, P. Doel, S. Ferraro, A. Font-Ribera, J. E. Forero-Romero, E. Gaztañaga, S. Gontcho A Gontcho, A. X. Gonzalez-Morales, G. Gutierrez, H. K. Herrera-Alcantar, K. Honscheid, C. Howlett, S. Juneau, R. Kehoe, D. Kirkby, T. Kisner, A. Kremin, C. Lamman, M. Landriau, L. Le Guillou, M. E. Levi, C. Magneville, M. Manera, A. Meisner, R. Miquel, J. Moustakas, A. Muñoz-Gutiérrez, A. D. Myers, S. Nadathur, G. Niz, H. E. Noriega, W. J. Percival, C. Poppett, F. Prada, I. Pérez-Ràfols, A. J. Ross, G. Rossi, L. Samushia, E. Sanchez, D. Schlegel, M. Schubnell, H. Seo, J. Silber, D. Sprayberry, G. Tarlé, M. Vargas-Magaña, B. A. Weaver, P. Zarrouk, R. Zhou, and H. Zou. Full-Shape analysis of the power spectrum and bispectrum of DESI DR1 LRG and QSO samples. *JCAP*, 2025(6):005, June 2025. [arXiv:2503.09714](#), [DOI], [ADS].
- [15] R. J. Bouwens, G. D. Illingworth, P. A. Oesch, M. Trenti, I. Labbé, L. Bradley, M. Carollo, P. G. van Dokkum, V. Gonzalez, B. Holwerda, M. Franx, L. Spitler, R. Smit, and D. Magee. UV Luminosity Functions at Redshifts $z \sim 4$ to $z \sim 10$: 10,000 Galaxies from HST Legacy Fields. *ApJ*, 803(1):34, April 2015. [arXiv:1403.4295](#), [DOI], [ADS].
- [16] Hakim Atek, Johan Richard, Jean-Paul Kneib, and Daniel Schaerer. The extreme faint end of the UV luminosity function at $z \sim 6$ through gravitational telescopes: a comprehensive assessment of strong lensing uncertainties. *MNRAS*, 479(4):5184–5195, October 2018. [arXiv:1803.09747](#), [DOI], [ADS].
- [17] R. J. Bouwens, P. A. Oesch, M. Stefanon, G. Illingworth, I. Labbé, N. Reddy, H. Atek, M. Montes, R. Naidu, T. Nanayakkara, E. Nelson, and S. Wilkins. New Determinations of the UV Luminosity Functions from $z \sim 9$ to 2 Show a Remarkable Consistency with Halo Growth and a Constant Star Formation Efficiency. *AJ*, 162(2):47, August 2021. [arXiv:2102.07775](#), [DOI], [ADS].
- [18] C. T. Donnan, D. J. McLeod, J. S. Dunlop, R. J. McLure, A. C. Carnall, R. Begley, F. Cullen, M. L. Hamadouche, R. A. A. Bowler, D. Magee, H. J. McCracken, B. Milvang-Jensen, A. Moneti, and T. Targett. The evolution of the galaxy UV luminosity function at redshifts $z \sim 8$ -15 from deep JWST and ground-based near-infrared imaging. *MNRAS*, 518(4):6011–6040, February 2023. [arXiv:2207.12356](#), [DOI], [ADS].
- [19] Yuichi Harikane, Masami Ouchi, Masamune Oguri, Yoshiaki Ono, Kimihiko Nakajima, Yuki Isobe, Hiroya Umeda, Ken Mawatari, and Yechi Zhang. A Comprehensive Study of Galaxies at $z \sim 9$ -16 Found in the Early JWST Data: Ultraviolet Luminosity Functions and Cosmic Star Formation History at the Pre-reionization Epoch. *ApJS*, 265(1):5, March 2023. [arXiv:2208.01612](#), [DOI], [ADS].

- [20] Rychard J. Bouwens, Mauro Stefanon, Gabriel Brammer, Pascal A. Oesch, Thomas Herard-Demanche, Garth D. Illingworth, Jorryt Matthee, Rohan P. Naidu, Pieter G. van Dokkum, and Ivana F. van Leeuwen. Evolution of the UV LF from $z \sim 15$ to $z \sim 8$ using new JWST NIRC*am* medium-band observations over the HUDF/XDF. *MNRAS*, 523(1):1036–1055, July 2023. [arXiv:2211.02607](#), [DOI], [ADS].
- [21] D. J. McLeod, C. T. Donnan, R. J. McLure, J. S. Dunlop, D. Magee, R. Begley, A. C. Carnall, F. Cullen, R. S. Ellis, M. L. Hamadouche, and T. M. Stanton. The galaxy UV luminosity function at $z \sim 11$ from a suite of public JWST ERS, ERO, and Cycle-1 programs. *MNRAS*, 527(3):5004–5022, January 2024. [arXiv:2304.14469](#), [DOI], [ADS].
- [22] Peter Behroozi, Charlie Conroy, Risa H. Wechsler, Andrew Hearin, Christina C. Williams, Benjamin P. Moster, L. Y. Aaron Yung, Rachel S. Somerville, Stefan Gottlöber, Gustavo Yepes, and Ryan Endsley. The Universe at $z \lesssim 10$: predictions for JWST from the UNIVERSEMACHINE DR1. *MNRAS*, 499(4):5702–5718, December 2020. [arXiv:2007.04988](#), [DOI], [ADS].
- [23] Mark Vogelsberger, Dylan Nelson, Annalisa Pillepich, Xuejian Shen, Federico Marinacci, Volker Springel, Rüdiger Pakmor, Sandro Tacchella, Rainer Weinberger, Paul Torrey, and Lars Hernquist. High-redshift JWST predictions from IllustrisTNG: dust modelling and galaxy luminosity functions. *MNRAS*, 492(4):5167–5201, March 2020. [arXiv:1904.07238](#), [DOI], [ADS].
- [24] Rahul Kannan, Volker Springel, Lars Hernquist, Rüdiger Pakmor, Ana Maria Delgado, Boryana Hadzhiyska, César Hernández-Aguayo, Monica Barrera, Fulvio Ferlito, Sownak Bose, Simon D. M. White, Carlos Frenk, Aaron Smith, and Enrico Garaldi. The MillenniumTNG project: the galaxy population at $z \geq 8$. *MNRAS*, 524(2):2594–2605, September 2023. [arXiv:2210.10066](#), [DOI], [ADS].
- [25] Christopher C. Lovell, Ian Harrison, Yuichi Harikane, Sandro Tacchella, and Stephen M. Wilkins. Extreme value statistics of the halo and stellar mass distributions at high redshift: are JWST results in tension with Λ CDM? *MNRAS*, 518(2):2511–2520, January 2023. [arXiv:2208.10479](#), [DOI], [ADS].
- [26] Jordan Mirocha and Steven R. Furlanetto. Balancing the efficiency and stochasticity of star formation with dust extinction in $z \gtrsim 10$ galaxies observed by JWST. *MNRAS*, 519(1):843–853, February 2023. [arXiv:2208.12826](#), [DOI], [ADS].
- [27] Charlotte A. Mason, Michele Trenti, and Tommaso Treu. The brightest galaxies at cosmic dawn. *MNRAS*, 521(1):497–503, May 2023. [arXiv:2207.14808](#), [DOI], [ADS].
- [28] Michael Boylan-Kolchin. Stress testing Λ CDM with high-redshift galaxy candidates. *Nature Astronomy*, 7:731–735, June 2023. [arXiv:2208.01611](#), [DOI], [ADS].
- [29] Hamsa Padmanabhan and Abraham Loeb. Alleviating the Need for Exponential Evolution of JWST Galaxies in $10^{10} M_{\odot}$ Haloes at $z \lesssim 10$ by a Modified Λ CDM Power Spectrum. *ApJL*, 953(1):L4, August 2023. [arXiv:2306.04684](#), [DOI], [ADS].
- [30] Priyank Parashari and Ranjan Laha. Primordial power spectrum in light of JWST observations of high redshift galaxies. *MNRAS*, 526(1):L63–L69, November 2023. [arXiv:2305.00999](#), [DOI], [ADS].
- [31] Avishai Dekel, Kartick C. Sarkar, Yuval Birnboim, Nir Mandelker, and Zhaozhou Li. Efficient formation of massive galaxies at cosmic dawn by feedback-free starbursts. *MNRAS*, 523(3):3201–3218, August 2023. [arXiv:2303.04827](#), [DOI], [ADS].
- [32] Umberto Maio and Matteo Viel. JWST high-redshift galaxy constraints on warm and cold dark matter models. *A&A*, 672:A71, April 2023. [arXiv:2211.03620](#), [DOI], [ADS].

- [33] Boyuan Liu and Volker Bromm. Accelerating Early Massive Galaxy Formation with Primordial Black Holes. *ApJL*, 937(2):L30, October 2022. [arXiv:2208.13178](#), [DOI], [ADS].
- [34] Matteo Biagetti, Gabriele Franciolini, and Antonio Riotto. High-redshift JWST Observations and Primordial Non-Gaussianity. *ApJ*, 944(2):113, February 2023. [arXiv:2210.04812](#), [DOI], [ADS].
- [35] Gert Hütsi, Martti Raidal, Juan Urrutia, Ville Vaskonen, and Hardi Veermäe. Did JWST observe imprints of axion miniclusters or primordial black holes? *Phys.Rev.D*, 107(4):043502, February 2023. [arXiv:2211.02651](#), [DOI], [ADS].
- [36] Yan Gong, Bin Yue, Ye Cao, and Xuelei Chen. Fuzzy Dark Matter as a Solution to Reconcile the Stellar Mass Density of High- z Massive Galaxies and Reionization History. *ApJ*, 947(1):28, April 2023. [arXiv:2209.13757](#), [DOI], [ADS].
- [37] Xuejian Shen, Mark Vogelsberger, Michael Boylan-Kolchin, Sandro Tacchella, and Rahul Kannan. The impact of UV variability on the abundance of bright galaxies at $z \geq 9$. *MNRAS*, 525(3):3254–3261, November 2023. [arXiv:2305.05679](#), [DOI], [ADS].
- [38] Jackson Sipple and Adam Lidz. The Star Formation Efficiency during Reionization as Inferred from the Hubble Frontier Fields. *ApJ*, 961(1):50, January 2024. [arXiv:2306.12087](#), [DOI], [ADS].
- [39] Anirban Chakraborty and Tirthankar Roy Choudhury. Modelling the star-formation activity and ionizing properties of high-redshift galaxies. *JCAP*, 2024(7):078, July 2024. [arXiv:2404.02879](#), [DOI], [ADS].
- [40] Jiten Dhandha, Anastasia Fialkov, Thomas Gessey-Jones, Harry T. J. Bevins, Sandro Tacchella, Simon Pochinda, Eloy de Lera Acedo, Saurabh Singh, and Rennan Barkana. Exploiting synergies between JWST and cosmic 21-cm observations to uncover star formation in the early Universe. *MNRAS*, 542(3):2292–2322, September 2025. [arXiv:2503.21687](#), [DOI], [ADS].
- [41] Pratika Dayal and Sambit K. Giri. Warm dark matter constraints from the JWST. *MNRAS*, 528(2):2784–2789, February 2024. [arXiv:2303.14239](#), [DOI], [ADS].
- [42] Hovav Lazare, Ely D. Kovetz, Kimberly K. Boddy, and Julian B. Munoz. First galaxy ultraviolet luminosity function limits on dark matter-proton scattering. *arXiv e-prints*, page arXiv:2510.10757, October 2025. [arXiv:2510.10757](#), [DOI], [ADS].
- [43] Souradeep Das, Ranjini Mondol, Abhijeet Singh, and Ranjan Laha. Dark Secrets of Baryons: Illuminating Dark Matter-Baryon Interactions with JWST. *arXiv e-prints*, page arXiv:2511.02906, November 2025. [arXiv:2511.02906](#), [DOI], [ADS].
- [44] Jared Barron, David Curtin, Hongwan Liu, Julian Munoz, and Sandip Roy. Constraining Dark Acoustic Oscillations with the High-Redshift UV Luminosity Function. *arXiv e-prints*, page arXiv:2512.01998, December 2025. [arXiv:2512.01998](#), [DOI], [ADS].
- [45] Mattéo Blamart, Adrian Liu, Robert Brandenberger, Julian B. Muñoz, and Bryce Cyr. UV Luminosity Functions from HST and JWST: A Possible Resolution to the High-Redshift Galaxy Abundance Puzzle and Implications for Cosmic Strings. *arXiv e-prints*, page arXiv:2512.09980, December 2025. [arXiv:2512.09980](#), [DOI], [ADS].
- [46] Alan H. Guth. Inflationary universe: A possible solution to the horizon and flatness problems. *Phys.Rev.D*, 23(2):347–356, January 1981. [DOI], [ADS].
- [47] A. D. Linde. A new inflationary universe scenario: A possible solution of the horizon, flatness,

- homogeneity, isotropy and primordial monopole problems. *Physics Letters B*, 108(6):389–393, February 1982. [\[DOI\]](#), [\[ADS\]](#).
- [48] A. A. Starobinsky. A new type of isotropic cosmological models without singularity. *Physics Letters B*, 91(1):99–102, March 1980. [\[DOI\]](#), [\[ADS\]](#).
- [49] A. Albrecht and P. J. Steinhardt. Cosmology for Grand Unified Theories with Radiatively Induced Symmetry Breaking. *Phys.Rev.Lett.*, 48(17):1220–1223, April 1982. [\[DOI\]](#), [\[ADS\]](#).
- [50] Neil Barnaby and Zhiqi Huang. Particle production during inflation: Observational constraints and signatures. *Phys.Rev.D*, 80(12):126018, December 2009. [arXiv:0909.0751](#), [\[DOI\]](#), [\[ADS\]](#).
- [51] Rajeev Kumar Jain, Pravabati Chingangbam, Jinn-Ouk Gong, L. Sriramkumar, and Tarun Souradeep. Punctuated inflation and the low CMB multipoles. *JCAP*, 2009(1):009, January 2009. [arXiv:0809.3915](#), [\[DOI\]](#), [\[ADS\]](#).
- [52] Minu Joy, Arman Shafieloo, Varun Sahni, and Alexei A. Starobinsky. Is a step in the primordial spectral index favoured by CMB data? *JCAP*, 2009(6):028, June 2009. [arXiv:0807.3334](#), [\[DOI\]](#), [\[ADS\]](#).
- [53] Dhiraj Kumar Hazra, Moumita Aich, Rajeev Kumar Jain, L. Sriramkumar, and Tarun Souradeep. Primordial features due to a step in the inflaton potential. *JCAP*, 2010(10):008, October 2010. [arXiv:1005.2175](#), [\[DOI\]](#), [\[ADS\]](#).
- [54] Vinícius Miranda, Wayne Hu, and Peter Adshead. Warp features in DBI inflation. *Phys.Rev.D*, 86(6):063529, September 2012. [arXiv:1207.2186](#), [\[DOI\]](#), [\[ADS\]](#).
- [55] Jens Chluba, Jan Hamann, and Subodh P. Patil. Features and new physical scales in primordial observables: Theory and observation. *International Journal of Modern Physics D*, 24(10):1530023, June 2015. [arXiv:1505.01834](#), [\[DOI\]](#), [\[ADS\]](#).
- [56] Daniel J. H. Chung, Edward W. Kolb, Antonio Riotto, and Igor I. Tkachev. Probing Planckian physics: Resonant production of particles during inflation and features in the primordial power spectrum. *Phys.Rev.D*, 62(4):043508, August 2000. [arXiv:hep-ph/9910437](#), [\[DOI\]](#), [\[ADS\]](#).
- [57] Neil Barnaby, Zhiqi Huang, Lev Kofman, and Dmitry Pogosyan. Cosmological fluctuations from infrared cascading during inflation. *Phys.Rev.D*, 80(4):043501, August 2009. [arXiv:0902.0615](#), [\[DOI\]](#), [\[ADS\]](#).
- [58] Kazuyuki Furuuchi. Excursions through KK modes. *JCAP*, 2016(7):008, July 2016. [arXiv:1512.04684](#), [\[DOI\]](#), [\[ADS\]](#).
- [59] Lauren Pearce, Marco Peloso, and Lorenzo Sorbo. Resonant particle production during inflation: a full analytical study. *JCAP*, 2017(5):054, May 2017. [arXiv:1702.07661](#), [\[DOI\]](#), [\[ADS\]](#).
- [60] Kazuyuki Furuuchi, Suvedha Suresh Naik, and Noel Jonathan Jobu. Large field excursions from dimensional (de)construction. *JCAP*, 2020(6):054, June 2020. [arXiv:2001.06518](#), [\[DOI\]](#), [\[ADS\]](#).
- [61] Suvedha Suresh Naik, Kazuyuki Furuuchi, and Pravabati Chingangbam. Particle production during inflation: a Bayesian analysis with CMB data from Planck 2018. *JCAP*, 2022(7):016, July 2022. [arXiv:2202.05862](#), [\[DOI\]](#), [\[ADS\]](#).
- [62] Mario Ballardini, Fabio Finelli, Federico Marulli, Lauro Moscardini, and Alfonso Veropalumbo. New constraints on primordial features from the galaxy two-point correlation function. *Phys.Rev.D*, 107(4):043532, February 2023. [arXiv:2202.08819](#), [\[DOI\]](#), [\[ADS\]](#).

- [63] Suvedha Suresh Naik, Pravabati Chingangbam, Saurabh Singh, Andrei Mesinger, and Kazuyuki Furuchi. Global 21 cm signal: a promising probe of primordial features. *JCAP*, 2025(5):038, May 2025. [arXiv:2501.02538](#), [DOI], [ADS].
- [64] Kanan Virkar, Suvedha Suresh Naik, and Pravabati Chingangbam. Minkowski Functionals of the 21 cm Signal as a Probe of Primordial Features. *arXiv e-prints*, page arXiv:2601.19450, January 2026. [arXiv:2601.19450](#), [DOI], [ADS].
- [65] Uroš Seljak. Analytic model for galaxy and dark matter clustering. *MNRAS*, 318(1):203–213, October 2000. [arXiv:astro-ph/0001493](#), [DOI], [ADS].
- [66] J. A. Peacock and R. E. Smith. Halo occupation numbers and galaxy bias. *MNRAS*, 318(4):1144–1156, November 2000. [arXiv:astro-ph/0005010](#), [DOI], [ADS].
- [67] Pratika Dayal, Andrea Ferrara, James S. Dunlop, and Fabio Pacucci. Essential physics of early galaxy formation. *MNRAS*, 445(3):2545–2557, December 2014. [arXiv:1405.4862](#), [DOI], [ADS].
- [68] Jaehong Park, Andrei Mesinger, Bradley Greig, and Nicolas Gillet. Inferring the astrophysics of reionization and cosmic dawn from galaxy luminosity functions and the 21-cm signal. *MNRAS*, 484(1):933–949, March 2019. [arXiv:1809.08995](#), [DOI], [ADS].
- [69] Peter S. Behroozi and Joseph Silk. A Simple Technique for Predicting High-redshift Galaxy Evolution. *ApJ*, 799(1):32, January 2015. [arXiv:1404.5299](#), [DOI], [ADS].
- [70] Piero Madau and Mark Dickinson. Cosmic Star-Formation History. *ARA&A*, 52:415–486, August 2014. [arXiv:1403.0007](#), [DOI], [ADS].
- [71] William H. Press and Paul Schechter. Formation of Galaxies and Clusters of Galaxies by Self-Similar Gravitational Condensation. *ApJ*, 187:425–438, February 1974. [DOI], [ADS].
- [72] A. Jenkins, C. S. Frenk, S. D. M. White, J. M. Colberg, S. Cole, A. E. Evrard, H. M. P. Couchman, and N. Yoshida. The mass function of dark matter haloes. *MNRAS*, 321(2):372–384, February 2001. [arXiv:astro-ph/0005260](#), [DOI], [ADS].
- [73] Diego Blas, Julien Lesgourgues, and Thomas Tram. The Cosmic Linear Anisotropy Solving System (CLASS). Part II: Approximation schemes. *JCAP*, 2011(7):034, July 2011. [arXiv:1104.2933](#), [DOI], [ADS].
- [74] Jérôme Martin and Robert Brandenberger. Dependence of the spectra of fluctuations in inflationary cosmology on trans-Planckian physics. *Phys.Rev.D*, 68(6):063513, September 2003. [arXiv:hep-th/0305161](#), [DOI], [ADS].
- [75] Richard Easther, Brian R. Greene, William H. Kinney, and Gary Shiu. Imprints of short distance physics on inflationary cosmology. *Phys.Rev.D*, 67(6):063508, March 2003. [arXiv:hep-th/0110226](#), [DOI], [ADS].
- [76] Xingang Chen, Richard Easther, and Eugene A. Lim. Generation and characterization of large non-Gaussianities in single field inflation. *JCAP*, 2008(4):010, April 2008. [arXiv:0801.3295](#), [DOI], [ADS].
- [77] Raphael Flauger, Liam McAllister, Enrico Pajer, Alexander Westphal, and Gang Xu. Oscillations in the CMB from axion monodromy inflation. *JCAP*, 2010(6):009, June 2010. [arXiv:0907.2916](#), [DOI], [ADS].

- [78] Akhil Antony, Fabio Finelli, Dhiraj Kumar Hazra, Daniela Paoletti, and Arman Shafieloo. A search for super-imposed oscillations to the primordial power spectrum in Planck and SPT-3G 2018 data. [arXiv e-prints](#), page arXiv:2403.19575, March 2024. [arXiv:2403.19575](#), [DOI], [ADS].